PAN
POLISH ACADEMY OF SCIENCES

Opto-Electronics Review

journal homepage: http://journals.pan.pl/opelre

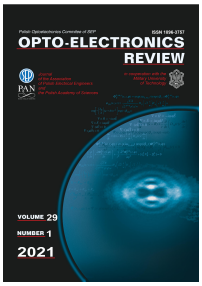

Barrier in the valence band in the nBn detector with an active layer from the type-II superlattice

M. Kopytko[a], E. Gomółka[a], T. Manyk[a*], K. Michalczewski[b], Ł. Kubiszyn[b], J. Rutkowski[a], P. Martyniuk[a]

[a] Institute of Applied Physics, Military University of Technology, 2. Kaliskiego St., 00-908 Warsaw, Poland
[b] Vigo System S.A., Poznańska 129/133, 05-850 Ożarów Mazowiecki, Poland

Article info

Article history:
Received 11 Sep. 2020
Received in revised form 8 Oct. 2020
Accepted 18 Oct 2020

Keywords:
infrared detector, T2SLs, superlattice, III-V materials, I-V characteristics.

Abstract

Numerical analysis of the dark current (I_d) in the type-II superlattice (T2SL) barrier (nBn) detector operated at high temperatures was presented. Theoretical calculations were compared with the experimental results for the nBn detector with the absorber and contact layers in an InAs/InAsSb superlattice separated AlAsSb barrier. Detector structure was grown using MBE technique on a GaAs substrate. The $k{\cdot}p$ model was used to determine the first electron band and the first heavy and light hole bands in T2SL, as well as to calculate the absorption coefficient.

The paper presents the effect of the additional hole barrier on electrical and optical parameters of the nBn structure. According to the principle of the nBn detector operation, the electrons barrier is to prevent the current flow from the contact layer to the absorber, while the holes barrier should be low enough to ensure the flow of optically generated carriers. The barrier height in the valence band (VB) was adjusted by changing the electron affinity of a ternary AlAsSb material. Results of numerical calculations similar to the experimental data were obtained, assuming the presence of a high barrier in VB which, at the same time, lowered the detector current responsivity.

1. Introduction

$A^{III}B^{V}$ materials, widely used in the construction of a superlattice (SL), have recently found application in the technology of infrared (IR) detectors due to a large possibility of regulating the energy gap size. The type-II superlattices (T2SLs) have advantages over the HgCdTe detectors [1,2]. The most important of them is a better stability, low tunnelling currents and suppression of the Auger generation-recombination. In case of materials with a comparable cut-off (λ_{co}) wavelength, significantly longer live times of minority carriers were obtained in the gallium free T2SL InAs/InAsSb compared to HgCdTe.

The T2SLs InAs/InAsSb superlattices are at the research and development stage and are less studied than the InAs/GaSb SL. The InAs/InAsSb SL material is characterized by a better controllability and a simpler manufacturability. The position of the conductivity band (CB) and the valence band (VB) in InAs/GaSb SL and InAs/InAsSb T2SLs are shown in Fig. 1.

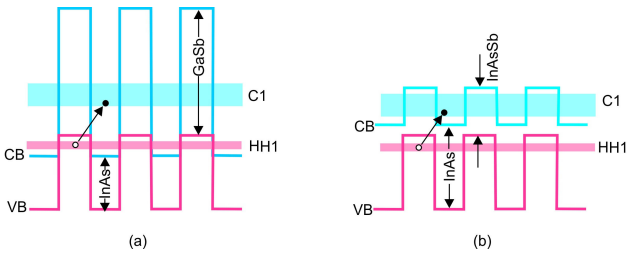

Fig. 1. Bandgap diagram of the superlatice: (a) InAs/GaSb and (b) InAs/InAsSb.

The fundamental properties of type-II InAs/InAsSb superlattices together with the bandgap engineering capability make this material available for the construction of a new class of IR detectors called barrier detectors [3-6]. An example of the barrier detector is the structure type nBn in which the barrier layer (BL) is sandwiched between an n-type semiconductor, which is a contact layer (CL), and an n-type absorber layer (AL). The nBn structure shows properties similar to a p-n junction and a photoresistor. Ideally, the barrier should

*corresponding author at: tetjana.manyk@wat.edu.pl
https://doi.org/10.24425/opelre.2021.135823

exist only in the conduction band, blocking the flow of majority carriers (electrons) which allow the unimpeded flow of holes (when there is no additional barrier in VB). Replacing the depletion layer by a CB barrier causes a change in the dark current density (J_d) through the suppression of Shockley-Reed generation. By generating a lower dark current, these detectors can operate at near room temperatures.

2. Experimental data, theoretical simulation and results

The epitaxial structure of nBn T2SL with the InAs/InAsSb absorber layer grown on a GaAs substrate using the RIBER molecular beam epitaxy system with effusion cells for Ga and In, and with valve cracked cells for As and Sb was obtained for the tests [7,8]. Growth rates were in situ calibrated according to the reflection high energy-electron diffraction (RHEED) system. The structural properties of applied T2SL layers and their stoichiometry (x_{Sb}) were determined by a diffractometer (PANalytical X'Pert). The under study nBn device consists of three basic layers. The BL was an $AlAs_{0.15}Sb_{0.85}$ material ($d = 0.1$ µm) while T2SL InAs (5.096 nm)/$InAs_{0.62}Sb_{0.38}$ (1.94 nm) $d = 3.17$ µm was used for AL and T2SL InAs (5.096 nm)/$InAs_{0.62}Sb_{0.38}$ (1.94 nm) $d = 1.1$ µm – for CL. T2SL layers were non-doped and had the n-type conductivity at a level of $1 \cdot 10^{22}$ m^{-3} at 230 K. Theoretical simulation of T2SL has been performed in the commercially program SimuApsys (T2SL modelling and nBn detector modelling were performed). The applied model took into account the influences of radiative recombination, Shockley-Read, Auger 1 and Auger 7. The presented theoretical simulation model includes both electrical and optical properties of T2SL. Using it, a detectors performance can be estimated.

Figure 2 shows experimental data of the current-voltage (I-V) characteristics for the nBn T2SL device operated at heigh temperatures. At temperatures obtained with thermoelectric coolers (of 210 and 230 K), relatively low current density values are observed. In the nBn T2SL device, the valence and conduction bands offsets are the parameters managing the transport in the heterostructure.

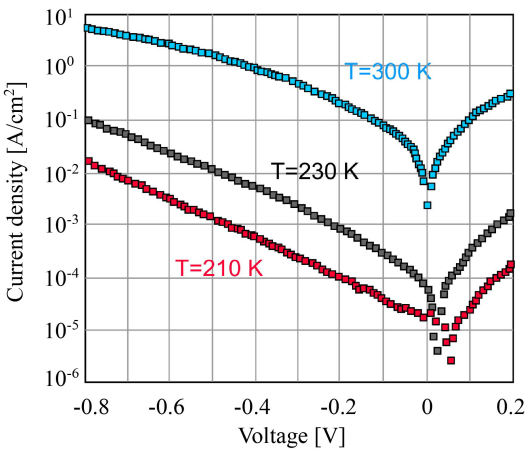

Fig. 2. The experimental I-V characteristics of the nBn detector at 210, 230 and 300 K.

Current-voltage plots indicate that there is an undesirable barrier in VB blocking the flow of carriers from the absorber. The low photovoltage with an open circuit appearing with a decreasing detector temperature is associated with a background radiation photocurrent. This is also confirmed by very low values of current responsivities measured at these temperatures (see Fig. 3). Current responsivities of 0.1 A/W are obtained by applying a very high bias voltage (above −1 V). This is the voltage that causes the barrier reduction in VB – so called "turn-on voltage". The AlAsSb barrier layer is much better aligned to the InAs/InAsSb SL absorber layer at room temperature. At 300 K the current responsivity at −0.5 V is more than an order of magnitude greater than at 210 K.

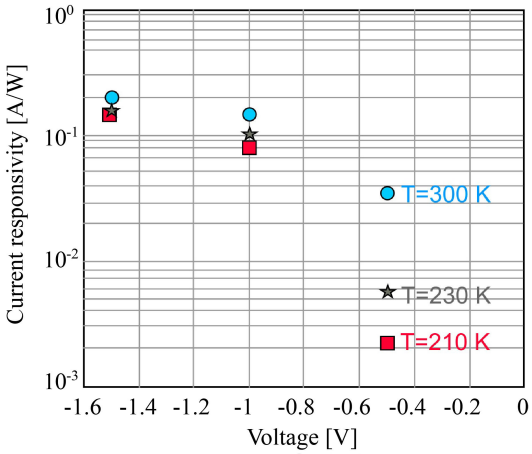

Fig. 3. Current responsivity vs. bias voltage for the nBn detector at high temperature.

Further analysis of J_d *vs.* temperature and determination of activation energy may give more details. The activation energy E_a matches the expression:

$$J_d \sim T^S e^{-\frac{E_a}{kT}}, \quad (1)$$

using the value of $S = 3$ for a low doped AL. In the above equation T is the temperature in Kelvin and k is the Boltzmann constant. Arrhenius plots of the dark current density at a bias of −0.2 V and −0.5 V are shown in Fig. 4.

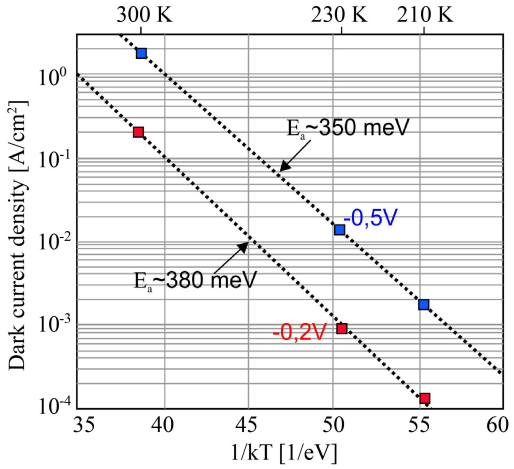

Fig. 4. Arrhenius plot of the dark current density at −0.2 V and −0.5 V for the nBn T2SL detector.

Determined activation energy for a voltage of −0.2 V equals 380 meV and is significantly higher than the InAs/InAsSb SL absorber energy gap. This value may correspond to the undesirable barrier height in VB. The existence of undesirable barriers can be explained by numerical modelling. The 8·8 $k·p$ model has been used which can theoretically model the absorption spectrum (absorption coefficient) and a cut-off wavelength of the absorber layer, based on the knowledge of the thickness of T2SL and the thickness of individual InAs and InAsSb materials in T2SL [9]. This model allows to determine the position of the conductivity and valence bands and to ensure a correct band alignment between BL and AL in the nBn T2SL detectors.

The good agreement was obtained by the theoretical modelling using a commercial platform SimuApsys. The simulation was conducted for T2SL with an InAs layer thicknesses of 5.096 nm and an $InAs_{0.62}Sb_{0.38}$ layer thickness of 1.94 nm. For example, the obtained λ_{co} (50%) = 6.7 μm at the temperature T = 230 K. The T2SL band structure of InAs (5.096 nm)/$InAs_{0.62}Sb_{0.38}$ (1.94 nm) was calculated in the temperature range of 230-300 K (these components thickness meets strain balancing conditions [10-12]). Also, probability functions showing that the holes are located in the InAsSb layer and electrons are in the InAs layer were calculated. It is known from theory that a transition is possible when the probability distribution functions overlap.

To determine the relative band alignment between each material specifies the CB and VB level as a bulk parameter for binary materials InAs, InSb, AlAs and AlSb. To derive the CB and VB level for an AlAsSb ternary alloy, a linear interpolation between binary materials can be used (AlSb and AsSb). The analysis for the position of the VB edge for a ternary material ($AlAs_{1-x}Sb_x$) is shown in Refs. 13-17. Reference 9 for $AlAs_{1-x}Sb_x$ ternary materials gives a bowing parameter value for the valence band (VB) of 1.71 eV.

The following SL parameters were used for modelling the nBn detectors: energy gap, electron affinity, electron and hole mass, recombination (radiative, Auger 1, Auger 7 and carriers lifetime SRH) absorption coefficient (Table 1).

Table 1.
SL parameters used in the nBn detectors simulation
(T = 230 K, λ = 4 μm).

Symbol	Quantity	Value
E_g	Energy gap	0.164 eV
χ	Electron affinity	4.892 eV
m_e/m_0	Electron mass	0.059
m_h/m_0	Hole mass	0.179
R_i	Radiative recombination coefficients	$3.07 \cdot 10^{-16}$ m^3s^{-1}
$\tau_{SRH\text{-}n}$	Electrons SRH lifetime	$100 \cdot 10^{-9}$ s
$\tau_{SRH\text{-}p}$	Holes SRH lifetime	$100 \cdot 10^{-9}$ s
τ_{A1}	Recombination coefficients Auger 1	$2.98 \cdot 10^{-39}$ m^3s^{-1}
τ_{A7}	Recombination coefficients Auger 7	$1.22 \cdot 10^{-39}$ m^3s^{-1}
α	Absorption coefficient	876 cm^{-1}

The theoretical analysis results of the optical generation of carriers indicate that the greatest absorption takes place in the detector active layer. Reflections were not included in our simulations.

The T2SL electron affinity was theoretically determined according to the method described in Ref. 18. For the ternary bulk material of AlAsSb, which occurs as a barrier, the following equation has been used to determine the electron affinity (χ):

$$\chi = \left| E_v - E_g \right|, \tag{2}$$

where E_v is the valence band energy, E_g is the band gap energy. Figure 5 shows the theoretical analysis of the current density at a reverse bias voltage equal to −0.2V and −0.4V as a function of the valence band offset (VBO) at the boundary between the barrier and the detector absorber.

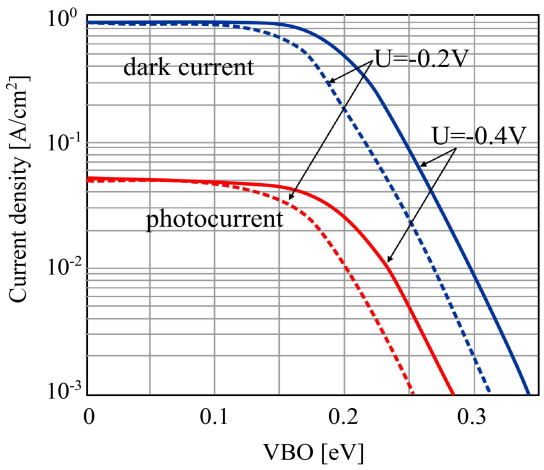

Fig. 5. Calculated current and photocurrent density at U = −0.2 V and −0.4 V as a function of VBO for the nBn detector operated at 230 K.

Changing the VBO causes changes in the device operation and in a deterioration in the detector quantum efficiency. An increase in VBO reduces the dark current density, but at the same time, the detector quantum efficiency decreases. At the polarization voltage U = −0.4 V, the barriers with a height lower than 0.2 eV do not limit the detector operation. At lower detector bias voltage values, this barrier height limit is lowered (0.1 eV). Due to the low values of the dark current in the tested detectors, we had to assume a VBO value of about 0.3 eV to match the experimental I-V characteristics.

Figure 6 shows, for example, the measured and theoretically calculated I-V characteristics for the nBn T2SL devices operated at 230 K.

The presence of a barrier in the VB obstructs the flow of holes. With an increase in the detector polarization in the reverse bias of about −0.4 V, the barrier decreases which results in a current responsivity increase. This also causes an increase in the dark current detector due to an increase in the minority carrier current. In our case, the correct band alignment between BL and AL was not obtained.

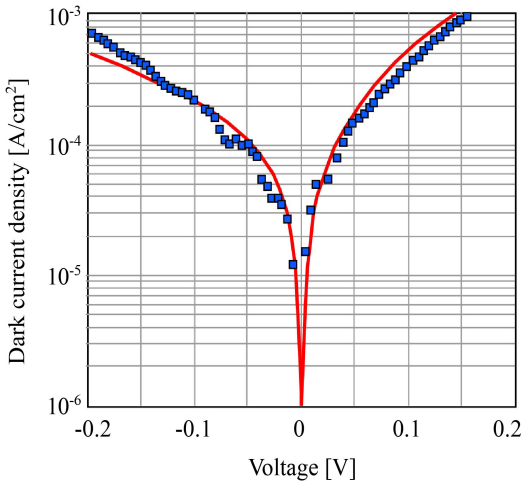

Fig. 6. Eksperimental data (points) and theoretical calculation (lines) of I-V characteristics of the nBn T2SL detector operated at 230 K.

3. Conclusions

The article presents the theoretical analysis of the performance of nBn T2SL (CL [InAs/InAsSb] - BL [AlAsSb] - AL [InAsSb]) barrier detectors operated at high temperatures. Results of the theoretical simulations were compared to the measured data for the obtained barrier detectors. Position of the VB edge for the ternary barrier materials (AlAsSb) was changed by correcting the electron affinity in the barrier layer (changing the bowing parameter). Good adjustment of the theoretical curves to the measured I-V characteristics of the nBn detector required the adoption of a high barrier in the valence band which decreased the detector current responsivity at low reverse bias voltage values. In further work the authors plan to use a three-component AlInSb alloy and a two-component AlSb alloy for BL as a potentially better suited material for InAs/InAsSb AL which will allow to increase the quantum efficiency of the device.

Acknowledgements

This work was supported by the funds GB/1/2018/205/2018/DA.

References

[1] Aytac, Y. *et al*. Effects of layer thickness and alloy composition on carrier lifetimes in mid-wave infra-red InAs/InAsSb superlattices. *Appl. Phys. Lett.* **105**, 022107 (2014). https://doi.org/10.1063/1.4890578

[2] Olson, B. *et al*. Identification of dominant recombination mechanisms in narrow-bandgap InAs/InAsSb type-II superlattices and InAsSb alloys. *Appl. Phys. Lett.* **103**, 052106 (2013). https://doi.org/10.1063/1.4817400

[3] White, M., 1983. *Infrared Detectors*. U.S. Patent 4,679,063.

[4] Klipstein, P., 2003. *Depletionless photodiode with suppressed dark current and method for producing the same*. U.S. Patent 7,795,640.

[5] Maimon, S. & Wicks, G. nBn detector, an infrared detector with reduced dark current and higher operating temperature. *Appl. Phys. Lett.* **89**, 151109 (2006). https://doi.org/10.1063/1.2360235

[6] Ting, D. Z.-Y. *et al*. Chapter 1 - Type-II Superlattice Infrared Detectors. in *Advances in Infrared Photodetectors* (eds. Gunapala, S. D., Rhiger, D. R. & Jagadish, C.) vol. 84 1–57 (Elsevier, 2011). https://doi.org/10.1016/B978-0-12-381337-4.00001-2

[7] Benyahia, D. *et al*. Low-temperature growth of GaSb epilayers on GaAs (001) by molecular beam epitaxy. *Opto-Electron. Rev.* **24**, 40–45 (2016).https://doi.org/10.1515/oere-2016-0007

[8] Benyahia, D. *et al*. Molecular beam epitaxial growth and characterization of InAs layers on GaAs (001) substrate. *Opt. Quant. Electron.* **48**, 428 (2016). https://doi.org/10.1007/s11082-016-0698-4

[9] Vurgaftman, I., Meyer, J. & Ram-Mohan, L. Band parameters for III-V compound semiconductors and their alloys. *J. Appl. Phys.* **89**, 5815–5875 (2001). https://doi.org/10.1063/1.1368156

[10] Birner, S. Modelling of semiconductor nanostructures and semiconductor-electrolyte interfaces. Ph.D. dissertation (Universität München, Germany, 2011).

[11] Chuang, Sh. L. *Physics of optoelectronic devices*. (Wiley, New York, 1995).

[12] Van de Walle, C. Band lineups and deformation potentials in the model-solid theory. *Phys. Rev. B* **39**, 1871–1883 (1989). https://doi.org/10.1103/PhysRevB.39.1871

[13] Kopytko, M. *et al*. Numerical Analysis of Dark Currents in T2SL nBn Detector Grown by MBE on GaAs Substrate. P*roceedings* **27**, 37 (2019), https://doi.org/10.3390/proceedings2019027037

[14] Hazbun, R. *et al*. Theoretical study of the effects of strain balancing on the bandgap of dilute nitride InGaSbN/InAs superlattices on GaSb substrates. *Infrared Phys. Technol.* **69**, 211–217 (2015). https://doi.org/10.1016/j.infrared.2015.01.023

[15] Livneh, Y. *et al*. *k-p* model for the energy dispersions and absorption spectra of InAs/GaSb type-II superlattices. *Phys. Rev. B* **86**, 235311 (2012). https://doi.org/10.1103/PhysRevB.86.235311

[16] Yu, P. & Cardona, M. *Fundamentals of semicon-ductors: Physics and materials properties*, 4th edn. (Springer, Heidelberg, 2010).

[17] Adachi, S. *Properties of group – IV, III-V and II-VI Semiconductors*. (Wiley, London, 2005).

[18] Manyk, T. *et al*. Method of electron affinity evaluation for the type-2 InAs/$InAs_{1-x}Sb_x$ superlattice. *J. Mater. Sci.* **55**, 5135–5144 (2020).https://doi.org/10.1007/s10853-020-04347-6